



Cite this: *Phys. Chem. Chem. Phys.*,  
2017, 19, 22141

# Spin dynamics of light-induced charge separation in composites of semiconducting polymers and PC<sub>60</sub>BM revealed using Q-band pulse EPR†

E. A. Lukina,<sup>ab</sup> E. Suturina,<sup>c</sup> E. Reijerse,<sup>d</sup> W. Lubitz<sup>d</sup> and L. V. Kulik<sup>ab</sup> 

Light-induced processes in composites of semiconducting polymers and fullerene derivatives have been widely studied due to their usage as active layers of organic solar cells. However the process of charge separation under light illumination – the key process of an organic solar cell is not well understood yet. Here we report a Q-band pulse electron paramagnetic resonance study of composites of the fullerene derivative PC<sub>60</sub>BM ([6,6]-phenyl-C<sub>61</sub>-butyric acid methyl ester) with different p-type semiconducting polymers regioregular and regiorandom P3HT (poly(3-hexylthiophene-2,5-diy)), MEH-PPV (poly[2-methoxy-5-(2-ethylhexyloxy)-1,4-phenylenevinylene]), PCDTBT (poly[N-9'-heptadecanyl-2,7-carbazole-alt-5,5-(4',7'-di-2-thienyl-2',1',3'-benzothiadiazole)]), PTB7 (poly({4,8-bis((2-ethylhexyl)oxy)benzo[1,2-b:4,5-b']dithiophene-2,6-diy}){3-fluoro-2-[(2-ethylhexyl)carbonyl]thieno[3,4-b]thiophenediy})), resulting in a detailed description of the in-phase laser flash-induced electron spin echo (ESE) signal. We found that in organic donor-acceptor composites the laser flash simultaneously induces species of two types: a polymer<sup>•+</sup>/fullerene<sup>•-</sup> spin-correlated polaron pair (SCPP) with an initial singlet spin state and (nearly) free polymer<sup>•+</sup> and fullerene<sup>•-</sup> species with non-equilibrium spin polarization. Species of the first type (SCPP) are well-known for polymer/fullerene blends and are usually associated with a charge-separated state. Also, spin polarization of long-living free species (polarons in deep traps) is affected by the laser flash, which is the third contribution to the flash-induced ESE signal. A protocol for extracting the in-phase ESE signal of the SCPP based on the dependence of the microwave nutation frequency on the strength of the spin coupling within the polaron pair was developed. Nutation experiments revealed an unusual pattern of the SCPP in RR-P3HT/PC<sub>60</sub>BM composites, from which the strength of the exchange interaction between the polymer<sup>•+</sup> and fullerene<sup>•-</sup> was extracted. In composites with low-efficient polymers the contribution of the SCPP to the in-phase ESE signal is high, while in composites with high-efficient polymers it is low. This finding can be used as a selection criterion of charge separation efficiency in the polymer/fullerene composites.

Received 1st June 2017,  
Accepted 26th July 2017

DOI: 10.1039/c7cp03680a

rs.c.li/pccp

<sup>a</sup> Voevodsky Institute of Chemical Kinetics and Combustion of Siberian Branch of Russian Academy of Sciences, Institutskaya 3, 630090 Novosibirsk, Russia.  
E-mail: chemphy@kinetics.nsc.ru; Tel: +7-383-3332297

<sup>b</sup> Novosibirsk State University, Pirogova 2, 630090 Novosibirsk, Russia

<sup>c</sup> School of Chemistry, University of Southampton, Highfield Campus, Southampton, UK

<sup>d</sup> Max Planck Institute for Chemical Energy Conversion, Stifst. 34-36,  
D-45470 Muelheim an der Ruhr, Germany

† Electronic supplementary information (ESI) available: ED EPR spectra of RR-P3HT/PC<sub>60</sub>BM composites in the dark and under continuous light illumination, ED flash-induced EPR spectra of RR-P3HT/PC<sub>60</sub>BM measured with pre-saturation at different temperatures, simulations of the nutation curves for tight SCPP RR-P3HT<sup>•+</sup>/PC<sub>60</sub>BM<sup>•-</sup> with different parameters of exchange and dipolar interactions, a model system for DFT calculations and computed *g*-factors of the positively charged polythiophene polaron as a function of a distance to a negative point charge, simulations of the extracted SCPP spectrum with a modified RR-P3HT<sup>•+</sup> *g*-tensor. See DOI: 10.1039/c7cp03680a

## Introduction

There is a rapid development in the field of organic photovoltaics and some commercial applications have already been described.<sup>1-6</sup> Power conversion efficiencies of organic solar cells typically lie in the range of 8–9%, the largest value obtained so far is 11.2%.<sup>7</sup> The active layer of organic solar cells is usually a bulk heterojunction (BHJ)<sup>1-6</sup> comprising a p-type semiconducting polymer as an electron donor<sup>8-11</sup> and a fullerene derivative as an electron acceptor,<sup>12</sup> although new promising materials, typically polycondensed heterocycles, have also been employed.<sup>13,14</sup> The key process in organic solar cell operation is the charge separation process that takes place in the active layer under light illumination.<sup>15-17</sup> Its mechanism is, however, not completely understood.<sup>18,19</sup>

The charge separation process in organic composites is mainly studied using transient absorption spectroscopy<sup>20,21</sup>

and time-resolved (TR) EPR.<sup>22–29</sup> The following model of the charge separation process has been developed using the results of these studies. After the active layer has absorbed light, an exciton is formed. This diffuses through the material until it decays to the ground state or reaches the donor–acceptor interface where the electron is transferred from the semiconducting polymer to the fullerene. Thereby an intermediate charge transfer (CT) state is formed. In the CT state electrons and holes are situated on the acceptor and the donor molecules, respectively, but they are still bound by strong Coulombic interactions. Hereafter the CT state separates into free charges with almost unity quantum yield in many polymer/fullerene blends. This description is rather simplified and, actually, the understanding of the charge separation mechanism at the organic donor/acceptor interface still remains a challenge.

One of the major problems of both transient absorption and time-resolved EPR is the difficulty of signal assignment, especially if the spectrum consists of many different contributions. In contrast, pulse EPR, in particular electron spin echo (ESE) spectroscopy, provides the opportunity to separate different contributions to the signal by varying microwave pulse sequences and pulse amplitudes. Thus, pulse EPR is a valuable technique in the investigation of the charge separation process in organic donor/acceptor composites. In such experiments the so-called flash-induced ESE signal is usually analyzed which is the difference of the ESE signals obtained with the same microwave pulse sequence obtained for a short Delay After the laser Flash ( $T_{\text{DAF}}$ ), and for sufficiently long  $T_{\text{DAF}}$ . It is assumed that all transient paramagnetic species decay for long  $T_{\text{DAF}}$  and only stable species remain. Previously, pulse X-band EPR spectroscopy was applied to studies of RR-P3HT (regio-regular poly(3-hexylthiophene)) and PC<sub>60</sub>BM ([6,6]-phenyl-C<sub>61</sub>-butyric acid methyl ester) or PC<sub>70</sub>BM ([6,6]-phenyl-C<sub>71</sub>-butyric acid methyl ester) composites, and the observed out-of-phase electron spin echo envelope modulation (ESEEM) was interpreted as a feature of a singlet-born spin-correlated polaron pair (SCPP) polymer<sup>•+</sup>/fullerene<sup>•-</sup>.<sup>30,31</sup> However, the nature of in-phase flash-induced signals is not yet completely understood.<sup>30–33</sup> Since for sufficiently selective microwave pulses in-phase flash-induced ESE is proportional to the magnetization change caused by the laser flash, its magnetic field dependence (echo-detected EPR spectrum) is expected to be similar to the TR EPR spectrum. It should be noted that the evolution of the TR EPR spectrum for RR-P3HT/PC<sub>60</sub>BM with the increase of  $T_{\text{DAF}}$  cannot be interpreted within the simple singlet-born SCRP framework.<sup>22</sup> Taken together these facts show that the spin dynamics in polymer/fullerene composites is more complex than it was suggested in the earlier singlet spin-correlated radical pair (SCRP) model,<sup>34</sup> which has been successfully applied to the photosynthetic charge separation process.<sup>35–43</sup>

Here we report a Q-band pulse electron paramagnetic resonance study of composites of the fullerene derivative PC<sub>60</sub>BM([6,6]-phenyl-C<sub>61</sub>-butyric acid methyl ester) with different conductive polymers (regioregular (RR) and regiorandom (RRa) P3HT (poly(3-hexylthiophene-2,5-diyl)), MEH-PPV (poly[2-methoxy-5-(2-ethylhexyloxy)-1,4-phenylenevinylene]), PCDTBT

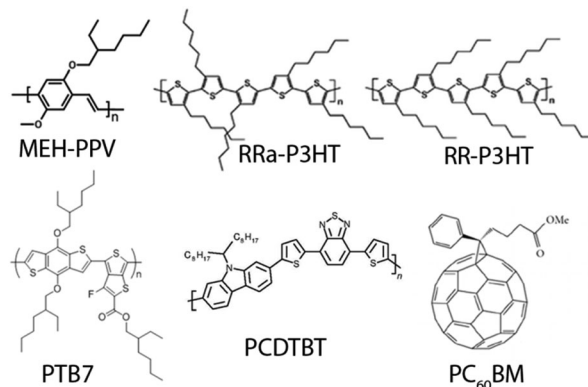


Fig. 1 Molecular structures of the substances used.

(poly[*N*-9'-heptadecanyl-2,7-carbazole-*alt*-5,5'-(4',7'-di-2-thienyl-2',1',3'-benzothiadiazole)]), PTB7 (poly{4,8-bis[(2-ethylhexyl)oxy]benzo[1,2-*b*:4,5-*b'*]dithiophene-2,6-diyl}{3-fluoro-2-[(2-ethylhexyl)carbonyl]thieno[3,4-*b*]thiophenediyl})) (see molecular structures in Fig. 1), resulting in a detailed description of the in-phase laser flash-induced electron spin echo (ESE) signal. Using different pulse sequences and the high spectral resolution obtained at the Q-band we were able to separate several contributions to this signal. We found that in organic donor–acceptor composites the laser flash induces not only a polymer<sup>•+</sup>/fullerene<sup>•-</sup> SCPP with an initial singlet spin state but also free or nearly free polymer<sup>•+</sup> and fullerene<sup>•-</sup> polaron species with non-equilibrium spin polarization, which can be either absorptive or emissive. These non-equilibrium polarized species are known to appear as a result of a separation of a geminate radical (polaron) pair to rather long distances (CIDEP mechanism)<sup>44,45</sup> or by polarization transfer from the SCRP to a third observer spin,<sup>46,47</sup> presumably, pre-existing polarons in deep traps. We also developed a protocol for suppressing the contribution of free species to the flash-induced ESE signal. Using this protocol we estimated the strength of the exchange interaction for the CT state RR-P3HT<sup>•+</sup>/PC<sub>60</sub>BM<sup>•-</sup>.

## Theory

Since a bulk heterojunction is intrinsically disordered, the precise description of the CT state in a polymer/fullerene composite would imply a broad distribution of distances between its parts, polymer<sup>•+</sup> and fullerene<sup>•-</sup>. This implies also a distribution of the parameters of the exchange and magnetic dipolar interactions. In the present study we consider a highly simplified model of this distribution consisting of only two subensembles. The first one (CT state) has a small fixed distance between polarons, a fixed exchange and dipolar interaction parameters and an initial singlet spin state; thus it can be treated as a SCPP. The second subensemble (separated charges) has a long distance between polarons and negligible strength of magnetic interactions between them. In this case a pure singlet RP is not observable in the ESE experiments. We assume, however, that these species carry non-equilibrium spin polarization. Initially, this is CIDEP with an A/E pattern, which

is gradually converted to Boltzmann polarization at longer  $T_{\text{DAF}}$  because of spin–lattice relaxation.

The theoretical description of a SCRPP was developed for the interpretation of photosynthetic reaction centers and is described in detail elsewhere.<sup>34,48,49</sup> Here we will briefly outline the main aspects of this theory and then describe the modifications necessary to apply it to the simulation of our ESE experiments.

The spin Hamiltonian of a polaron pair contains the Zeeman interactions of both polarons with the external magnetic field, as well as the dipole and exchange interactions between polarons:<sup>49</sup>

$$H = \mu_{\text{B}}g_{1\text{eff}}B_0S_{1z} + \mu_{\text{B}}g_{2\text{eff}}B_0S_{2z} + J\left(\frac{1}{2} - 2S_1S_2\right) + \frac{1}{2}D(3\cos^2\xi - 1)\left(S_z^2 - \frac{1}{3}S^2\right) \quad (1)$$

Here  $\mu_{\text{B}}$  is the Bohr magneton,  $B_0$  is the spectrometer magnetic field,  $g_{1\text{eff}}$  and  $g_{2\text{eff}}$  are the effective  $g$ -factors of polarons 1 and 2, respectively,  $S_1$  and  $S_2$  are their spin operators,  $S$  denotes the total spin operator  $S_1 + S_2$ ,  $J$  is the exchange coupling,  $D$  is the dipolar coupling,  $\xi$  is the angle between the line connecting the polarons in the pair and the external magnetic field. The hyperfine coupling in organic photovoltaic materials is often negligible due to the strong delocalization of the spins and charges.

The spin centers in both polymers and fullerenes have anisotropic  $g$ -tensors, therefore the effective  $g$ -factor is determined as

$$g_{1,2\text{eff}} = g_{1,2x}\sin^2\theta_{1,2}\cos^2\varphi_{1,2} + g_{1,2y}\sin^2\theta_{1,2}\sin^2\varphi_{1,2} + g_{1,2z}\cos^2\theta_{1,2}, \quad (2)$$

where  $g_{1,2(x,y,z)}$  are the principal components of the  $g$ -tensor,  $\theta_{1,2}$  and  $\varphi_{1,2}$  are the angles characterizing the orientation of the molecular frame with respect to the magnetic field orientation (the  $z$ -axis of the laboratory frame). In the absence of interactions between spins 1 and 2 their resonance frequencies are  $\omega_1 = \mu_{\text{B}}g_{1\text{eff}}B_0$  and  $\omega_2 = \mu_{\text{B}}g_{2\text{eff}}B_0$ .

The eigenvectors and eigenvalues of the spin Hamiltonian (1) are

$$\begin{aligned} |1\rangle &= |T_+\rangle & E_1 &= -J + \frac{1}{2}d + \omega \\ |2\rangle &= \cos\psi|S\rangle + \sin\psi|T_0\rangle & E_2 &= -\frac{1}{2}d + \Omega \\ |3\rangle &= -\sin\psi|S\rangle + \cos\psi|T_0\rangle & E_3 &= -\frac{1}{2}d - \Omega \\ |4\rangle &= |T_-\rangle & E_4 &= -J + \frac{1}{2}d - \omega \end{aligned} \quad (3)$$

where

$$\omega = \frac{1}{2}(\omega_1 + \omega_2), \quad Q = \frac{1}{2}(\omega_1 - \omega_2), \quad d = D\left(\cos^2\xi - \frac{1}{3}\right), \\ \Omega^2 = \left(J + \frac{1}{2}d\right)^2 + Q^2, \quad tg2\psi = \frac{2Q}{2J + d}$$

The allowed EPR transition energies are:

$$\begin{aligned} \omega_{12} &= \omega - \Omega \cdot \text{sign}(tg2\psi) - (J - d) \\ \omega_{34} &= \omega - \Omega \cdot \text{sign}(tg2\psi) + (J - d) \\ \omega_{13} &= \omega + \Omega \cdot \text{sign}(tg2\psi) - (J - d) \\ \omega_{24} &= \omega + \Omega \cdot \text{sign}(tg2\psi) + (J - d) \end{aligned} \quad (4)$$

The sign function in the above equations is necessary for the correct assignment of the transition frequencies but it is lacking in previous treatments. It is assumed that microwave pulses are selective and that they excite only one allowed transition. This transition was treated as spin 1/2 with an effective gyromagnetic ratio  $\gamma_{\text{eff}} = \sqrt{2}\gamma_0 \sin\psi$  for the  $1 \leftrightarrow 2$  and  $2 \leftrightarrow 4$  transitions and  $\gamma_{\text{eff}} = \sqrt{2}\gamma_0 \cos\psi$  for the  $1 \leftrightarrow 3$  and  $3 \leftrightarrow 4$  transitions, where  $\gamma_0$  is the free electron gyromagnetic ratio. Every transition is broadened by a Gaussian function. We took into account that two radicals in the pair have different line widths and therefore calculated the line width of each individual line according to the relative contributions of the transition moments of polaron 1 and polaron 2 as

$$W_{ij} = W_1|\langle i|S_{1x}|j\rangle|^2 + W_2|\langle i|S_{2x}|j\rangle|^2, \quad (5)$$

where  $W_1$  and  $W_2$  are the individual line widths of polarons 1 and 2.

Thus we obtained

$$\begin{aligned} W_{12} &= W_{34} = [W_1(\cos\psi - \sin\psi)^2 + W_2(\cos\psi + \sin\psi)^2]/2 \\ W_{13} &= W_{24} = [W_1(\cos\psi + \sin\psi)^2 + W_2(\cos\psi - \sin\psi)^2]/2. \end{aligned} \quad (6)$$

For the case of a negligible interaction between spins ( $\psi = \pi/4$ ) the empirical relation (6) ensures that transitions belonging to the first polaron have the linewidth  $W_1$  and transitions of the second polaron have the linewidth  $W_2$ . For the case of strong spin coupling ( $\psi = 0$ ) eqn (6) ensures an average linewidth.

The initial level population (upon charge separation) was zero for levels 1 and 4,  $\cos^2\psi$  for level 2 and  $\sin^2\psi$  for level 3.

The ESE signal of the pair of non-interacting polarons was calculated using a similar approach. The difference from the SCPP calculation was the assumption  $J = 0$ ,  $D = 0$  and the appropriate initial population of the spin levels, representing longitudinal magnetization for spin of each polaron with equal magnitude and different sign (A/E polarization).

The line intensity of the ESE signal in  $t_{\text{p}}-\tau-2t_{\text{p}}-\tau$ -echo is the product of the population difference of the levels, the transition probability and  $\sin^3\alpha$ , where  $\alpha$  is the rotation angle of the first pulse  $\alpha = t_{\text{p}}\omega_1\langle S_x \rangle$ , in which  $t_{\text{p}}$  is a pulse length,  $\omega_1 = \gamma_0 B_1$  with  $B_1$  denoting the microwave amplitude,  $\langle S_x \rangle$  is  $\sin\psi$  for the  $1 \leftrightarrow 2$  and  $2 \leftrightarrow 4$  transitions and  $\cos\psi$  for the  $1 \leftrightarrow 3$  and  $3 \leftrightarrow 4$  transitions.<sup>50</sup> For the case of a negligible interaction between spins the maximum echo intensity is observed for  $t_{\text{p}}\omega_1 = \pi/2$ .

The nutation experiment with a pulse sequence  $\beta-T-t_{\text{p}}-\tau-2t_{\text{p}}-\tau$ -echo can be simulated using the same model as described above. The first microwave pulse with variable length changes

the level populations as follows

$$\begin{aligned}
 (P_2 - P_1) &\rightarrow (P_2 - P_1) \cos(\sqrt{2}\beta \sin \psi) \\
 (P_4 - P_2) &\rightarrow (P_4 - P_2) \cos(\sqrt{2}\beta \sin \psi) \\
 (P_4 - P_3) &\rightarrow (P_4 - P_3) \cos(\sqrt{2}\beta \cos \psi) \\
 (P_3 - P_1) &\rightarrow (P_3 - P_1) \cos(\sqrt{2}\beta \cos \psi)
 \end{aligned}
 \tag{7}$$

where  $\beta$  is the turning angle of the nutation pulse for isolated spin  $S = 1/2$ . The influence of the following two-pulse sequence can be calculated as described above. Thus we calculated the transition frequencies for all possible transitions in the spectrum, then took into account line broadening with the line-width determined as in eqn (6) and calculated the contribution of each line to the signal intensity at the chosen  $g$ -value. The extracted signal of the SCPP was determined as a difference of the ESE signal calculated with a strong pulse and the ESE calculated with a weak pulse, multiplied by  $2\sqrt{2}$ , according to the above protocol.

In each case the ESE signal for a polyoriented ensemble of SCPPs was obtained by averaging over the spatial orientations of the  $g$ -tensors. For the case of non-zero dipolar interactions averaging over the angle  $\xi$  was performed. All distributions were uncorrelated. We assume that hopping of the charges is slow compared to the duration of the microwave pulse sequence, so all magnetic parameters are constant.

## Experimental procedures

### Sample preparation

Regioregular and regiorandom P3HT (poly(3-hexylthiophene-2,5-diyl)), MEH-PPV (poly[2-methoxy-5-(2-ethylhexyloxy)-1,4-phenylenevinylene]), PCDTBT (poly[*N*-9'-heptadecanyl-2,7-carbazole-*alt*-5,5-(4',7'-di-2-thienyl-2',1',3'-benzothiadiazole)]), PTB7 (poly({4,8-bis[(2-ethylhexyl)oxy]benzo[1,2-*b*:4,5-*b'*]dithiophene-2,6-diyl}{3-fluoro-2-[(2-ethylhexyl)carbonyl]thieno[3,4-*b*]thiophenediyl})) and PC<sub>60</sub>BM ([6,6]-phenyl-C<sub>61</sub>-butyric acid methyl ester) (see molecular structures in Fig. 1) were purchased from Sigma Aldrich and used without further purification. One of the semiconducting polymers and PC<sub>60</sub>BM (weight ratio 1 : 1) were dissolved in chlorobenzene (concentration of each substance approximately 6 mg ml<sup>-1</sup>) and mixed using an ultrasonic mixer (QSonica Microson XL2000). Several freeze-pump-thaw cycles were performed, then the solvent was evaporated to form a composite film on the inner wall of a quartz sample tube (o.d. 2.8 mm). Then samples were annealed at 10<sup>-2</sup> Torr at 150 °C for about 10 minutes. This was done to remove traces of oxygen from the composite, which act as deep trap for polarons. The intensity of the dark EPR signal of these samples did not increase upon exposure to air at room temperature. This testifies that the composite is stable under ambient conditions, and sealing of the samples is not necessary.

### Pulse EPR experiments

EPR measurements were performed on a pulse Q-band Bruker ELEXSYS E580 EPR spectrometer (microwave frequency close

to 34 GHz) at the Max Planck Institute for Chemical Energy Conversion, Muelheim an der Ruhr, Germany. The spectrometer is equipped with a homebuilt TE011 microwave cavity<sup>51</sup> and a cryogen-free closed-cycle cryostat (Cryogenic Limited) employing a PT415 Cryomech Inc pulse tube cryocooler (1.5 W @ 4 K) maintaining a stable low temperature during long-time experiments. If not otherwise specified, the measurements were done at 40 K. This low temperature was used to ensure slow charge hopping after initial light-induced charge separation.

Light excitation was realized using an Innolas SpitLight 600 OPO laser system (700 nm, flash duration 5 ns, repetition rate 10 Hz, about 1 mJ light intensity reaching the sample) for all samples. The light absorption of the studied composites is relatively low in the infrared region, therefore the laser light penetrates deep into the sample and the resulting spatial distribution of light-induced species is expected to be homogeneous. Changing pulse excitation wavelength to 532 nm did not affect the resulting ED EPR spectral shape and nutation pattern, only signal intensity was varied. For continuous light illumination laser operating at 532 nm was used.

The following microwave pulse sequences were used in the experiments:

1. A two-pulse sequence was applied to form the ESE signal at a certain  $T_{\text{DAF}}$ .
2. An additional microwave pulse was added before the laser flash in order to turn the magnetization of stable species to the  $XY$  plane of the rotating frame and thus make its contribution to the resulting ESE signal zero. Amplitude and the duration of the first pulse were chosen so that the ESE signal without laser flash is zero.
3. For the measurements of ESE nutations the following pulse sequence was used: after the laser flash and delay  $T_{\text{DAF}}$  a microwave pulse with variable length  $t$  was applied. After a fixed delay time  $T$  the two-pulse sequence was applied for the detection of the echo.

Turning angles of all microwave pulses are related to separated polarons with negligible interactions with other electron spins. This situation occurs at long  $T_{\text{DAF}}$  when the flash-generated SCPPs either recombined or dissociated. The phase of ESE was tuned by the two-pulse ESE signal at long  $T_{\text{DAF}}$ , for which pure in-phase ESE is expected. In all experiments out-of-phase ESE amplitude was negligibly small.

## Results and discussion

### RR-P3HT/PC<sub>60</sub>BM composite

We measured the Q-band ED EPR spectra of RR-P3HT/PC<sub>60</sub>BM in the dark and under continuous light illumination (Fig. S1, ESI†). The obtained spectrum consists of two well-separated peaks, the peaks at a low and a high  $g$ -factor belong to PC<sub>60</sub>BM<sup>•-</sup> and RR-P3HT<sup>•+</sup>, respectively. The signal in the dark appears due to the presence of polaron species trapped in the defects; light irradiation generates long-living thermalized polarons that contribute to the spectrum. The Q-band in-phase light-induced ED EPR spectrum of RR-P3HT/PC<sub>60</sub>BM was determined as a

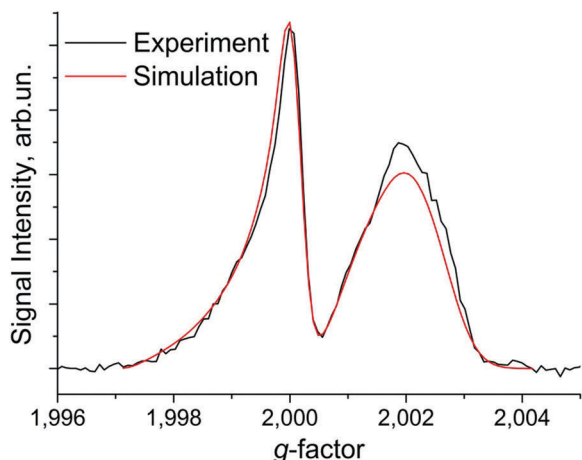


Fig. 2 Light-induced ED EPR spectrum of RR-P3HT/PC<sub>60</sub>BM determined as a difference between the spectrum measured under laser flashes without synchronization between laser flashes and the microwave pulse sequence and a spectrum measured in the dark after the laser light was turned off (red line). The measurements were done using the two-pulse sequence (Scheme 1). The spectrum was simulated using parameters of polaron species summarized in Table 1 and zero magnetic interactions between polarons (black line).

difference of the spectrum recorded under continuous unsynchronized laser flash illumination and the spectrum measured after the light was turned off (Fig. 2). The ESE signal of the thermalized polarons accumulated after many laser flashes is measured in this experiment; this spectrum is almost equal to that under continuous light irradiation meaning that it also belongs to thermalized long-living polarons. It should not be confused with the flash-induced ED EPR, in which the change in the ESE intensity caused by a single laser flash is measured.

We measured the flash induced ED EPR spectra of the RR-P3HT/PC<sub>60</sub>BM composite with  $T_{\text{DAF}} = 300$  ns and 99 ms delays between the excitation laser flash and the microwave pulse sequence. The spectra of RR-P3HT<sup>•+</sup> and PC<sub>60</sub>BM<sup>•-</sup> at the Q-band are clearly separated, the low  $g$ -factor and the high  $g$ -factor peaks correspond to fullerene and polymer polaron signals, respectively (Fig. 3). The spectrum with  $T_{\text{DAF}} = 99$  ms is similar to that of thermalized free polarons, implying that at such a long  $T_{\text{DAF}}$  all flash-induced species either recombined or thermalized.

The difference between the spectra at  $T_{\text{DAF}} = 300$  ns and 99 ms corresponds to the flash-induced signal (Fig. 4), which has emissive polarization at a high  $g$ -factor and very weak absorptive polarization at a low  $g$ -factor, similar to the previously observed flash-induced ED EPR spectra in composites of semiconducting polymers and fullerenes.<sup>30–33</sup> This signal presumably comprises both ESE of the light-induced species and the changes in the signal of long-living polarons. In order to separate these two contributions we applied an additional microwave pulse prior to the laser flash, which turns the magnetization of the long-living polarons into the XY plane and therefore suppresses their ESE signal (Scheme 2). The ESE signal of the flash-induced species without contribution of the long-living polarons is presented in Fig. 5.

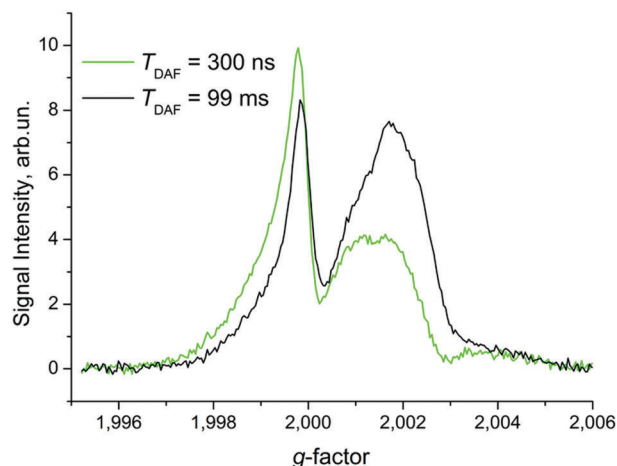


Fig. 3 Echo-detected EPR spectra of RR-P3HT/PC<sub>60</sub>BM measured with  $T_{\text{DAF}} = 300$  ns and 99 ms (green and black lines, respectively). A two-pulse microwave sequence with selective pulses and  $\tau = 400$  ns was used (Scheme 1).

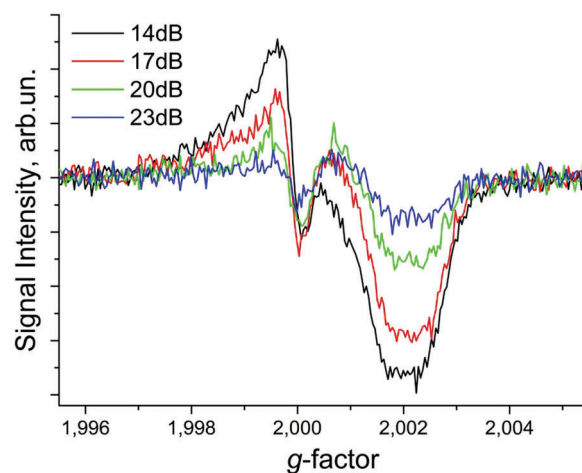
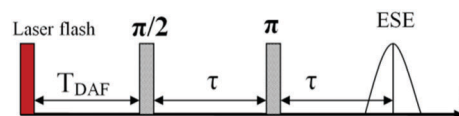


Fig. 4 Echo-detected flash-induced (determined as a difference of spectra measured with  $T_{\text{DAF}} = 300$  ns and 99 ms, pulse sequence 1) EPR spectra of RR-P3HT/PC<sub>60</sub>BM measured with different microwave power settings. The two-pulse microwave sequence with selective pulses (duration of the first pulse 100 ns) and  $\tau = 400$  ns was used. The numbers in the figure indicate the microwave attenuation level. Attenuation of 14 dB corresponds to the maximum ESE signal of the separated polarons.

The influence of the laser flash on the long-living free species (Fig. 6) was determined by subtraction of the pre-saturated flash induced spectra (measured according to Scheme 2) from the regular flash induced spectra (measured according to Scheme 1). The pre-saturation pulse suppresses the long-living magnetization but it does not affect the flash-induced species. Therefore the



Scheme 1 Two-pulse sequence.

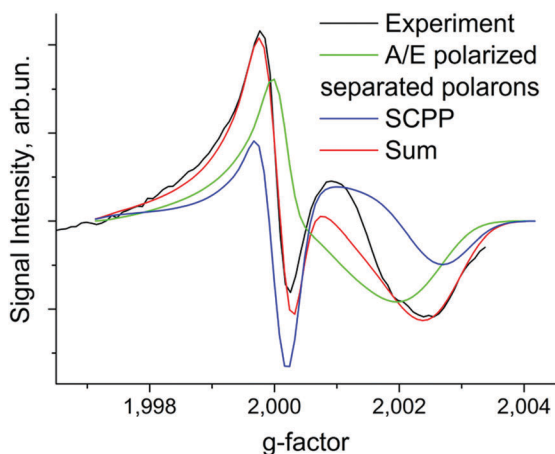
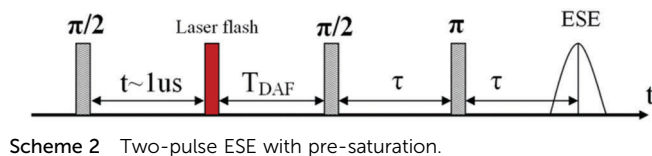


Fig. 5 Echo detected flash-induced EPR spectrum RR-P3HT/PC<sub>60</sub>BM measured with pre-saturation (black line). The pre-saturating microwave pulse was applied 1  $\mu$ s before the laser flash and a two-pulse microwave sequence with selective pulses and  $\tau = 400$  ns was used for detection (Scheme 2). Green and blue lines show simulated curves for A/E polarized separated polarons and SCPPs, respectively; the red line shows their sum. The simulation was done using the parameters of polaron species summarized in Table 1, assuming a dipolar interaction of 5 MHz and an exchange interaction of 3 MHz for SCPPs and zero magnetic interactions for A/E polarized separated polarons.

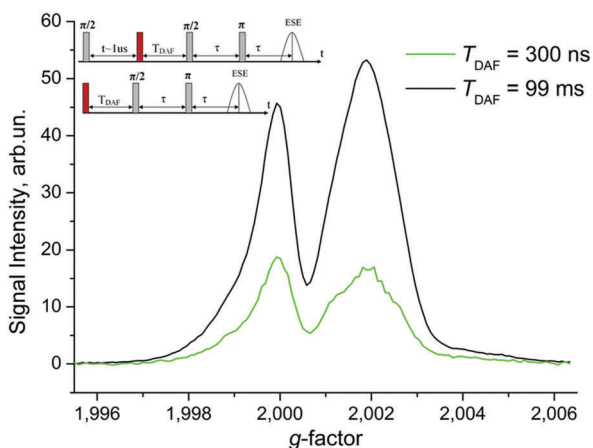


Fig. 6 Laser flash influence on long-living polarons of the EPR spectrum of the RR-P3HT/PC<sub>60</sub>BM composite. Spectra were determined as a difference between signals measured using the two pulse sequences shown in the inset with  $T_{\text{DAF}} = 300$  ns (green line) and  $T_{\text{DAF}} = 99$  ms (black line).

contribution of flash-induced species disappears after subtraction. As can be seen in Fig. 5 the laser flash significantly reduces the ESE signal of long-living polarons. The reason for this is not clear at present. One possibility is a polaron spin polarization change caused by exciton quenching by this polaron.

Exciton quenching on polarons is an important loss mechanism in polymer/fullerene OPV devices.<sup>52,53</sup> Presumably, it involves electron transfer from the exciton to a positive polaron or from a negative polaron to the exciton. The change in electron spin polarization during this process cannot be excluded, although it has not been reported to date. The other possible mechanism of polaron spin depolarization is bi-polaron formation observed at high concentrations of the polarons on polymer molecules.<sup>54</sup> This scenario implies that after the laser flash the concentration of polarons increases and a significant part of these form bi-polarons that are EPR silent, while at long  $T_{\text{DAF}}$  the charge concentration decreases due to recombination and most bi-polarons separate into free charges. The third possibility is partial interconversion of singlet excitons to triplet excitons before they dissociate at the donor acceptor interface, and transfer of spin polarization from triplet excitons to polarons. Such a process is known for stable radicals in organic matrices.<sup>55</sup> The origin of stable polaron depolarization is unclear for our case, but it seems not to be related to the CT state at the donor-acceptor interface. For this reason we did not analyze this effect further but suppressed it by our data treatment.

Even with pre-saturation of long-living polarons the ESE signal of flash-induced species (Fig. 5) consists of at least two contributions. During the charge separation process short-lived SCPPs with significant magnetic interactions between polarons are formed. This suggestion is supported by the non-uniform dependence of the flash-induced spectra on microwave power (Fig. 4). The ESE signal of the SCPP depends on microwave power differently than that of the free species with spin  $S = 1/2$ , which gives the opportunity to separate electron spin echo signals of different species.

As mentioned above we assume that the overall ESE signal at small  $T_{\text{DAF}}$  is a superposition of the contributions from the CT state and the separated polarons. We assume also that at long  $T_{\text{DAF}}$  the CT state either recombines or dissociates. Therefore, for  $T_{\text{DAF}} = 99$  ms only separated polarons contribute to the ESE signal. Under these assumptions it is possible to filter out the contribution of separated polarons from the mixture of ESE signals using the following protocol for the experimental data treatment:

1. We choose two values of the microwave amplitude for the primary ESE sequence with selective microwave pulses:  $A_1$  that is optimal for separated polarons (the maximal ESE signal at  $T_{\text{DAF}} = 99$  ms) and  $A_2 = A_1/2$  which corresponds to 6 dB higher microwave power attenuation than that for  $A_1$ . If the microwave amplitude is twice lower, the magnetization turning angles are also two times reduced. According to the Theory section the ESE intensity for separated polarons in this case scales by  $1/2\sqrt{2}$  compared to its maximum value, which corresponds to the  $\pi/2$  turning angle for the first pulse.

2. We measure four echo-detected EPR spectra with a two-pulse sequence with selective microwave pulses. Two of these spectra are recorded with optimal microwave power:  $S(T_{\text{DAF}} = 99$  ms,  $A_1)$ ,  $S(\text{short } T_{\text{DAF}}, A_1)$ . The other two spectra are recorded with reduced microwave power but with the same pulse length:  $S(T_{\text{DAF}} = 99$  ms,  $A_2)$ ,  $S(\text{short } T_{\text{DAF}}, A_2)$ .

3. We determine the coefficient  $K$  that describes how the signal of separated polarons changes with the decrease of the microwave power for the condition  $S(T_{\text{DAF}} = 99 \text{ ms}, A_2) - K \times S(T_{\text{DAF}} = 99 \text{ ms}, A_1) = 0$ . The experimental value of  $K$  is not exactly equal to  $1/2\sqrt{2}$  because of some uncertainty in the choice of  $A_1$ .

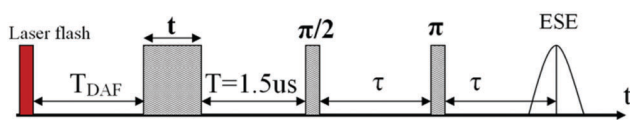
4. We subtract two spectra measured at short  $T_{\text{DAF}}$  with this coefficient  $K$  and thus cancel out the contribution of separated polarons to the ESE signal. Only the signal of the SCPP is left:  $S(\text{short } T_{\text{DAF}}, A_2) - K \times S(\text{short } T_{\text{DAF}}, A_1) = \text{CT state spectrum}$ .

It should be noted that the signal of the CT state is slightly distorted by this protocol: the stronger is the deviation of the particular SCPP from the weak coupling limit, the stronger is its contribution to the processed signal. Further such signal will be referred to as “extracted SCPP signal”. Thus, the extracted SCPP signal is decreased at the edges of the EPR spectrum, because these correspond to a larger difference of the Zeeman frequency of the spins constituting the pair, and consequently, to a smaller extent of spin coupling (the angle of singlet–triplet mixing  $\psi$  is close to  $\pi/4$ ). Analogously, by subtraction of the signals measured with different microwave power for short  $T_{\text{DAF}}$  (step 4 of the above protocol), it is possible to filter out the signal of isolated polarons and extract the SCPP contribution not only in the ED EPR spectrum, but also in ESE nutation (Scheme 3). This approach still works if the following conditions are fulfilled: the measured signal is primary ESE and amplitude of all other pulses (the first microwave pulse for the case of nutation experiment) is the same in the set of measurements. The scaling coefficient  $K$  can be determined at step 3 of the above protocol from two-pulse ESE for long  $T_{\text{DAF}}$  (measurements at two different microwave powers); this two-pulse ESE sequence should be the same as the detection unit in the nutation sequence (the second and the third pulses in Scheme 3).

The process of the extraction of this signal from experimental data is illustrated in Fig. 7. Under our conditions the precision of the experimental determination of optimal microwave power is about 1 dB, which translates in deviation of the scaling coefficient  $K$  from the theoretical value  $1/2\sqrt{2}$ . The value of  $K$  was in the range 0.3–0.4 in our experiments.

The distortion of the shape of the echo-detected EPR spectrum of the SCPP caused by the extraction procedure is illustrated for the simulated SCPP spectra in Fig. S2 (ESI<sup>†</sup>).

In Fig. 8 we show the extracted signal of the SCPP for RR-P3HT/PC<sub>60</sub>BM. We can see that the extracted SCPP signal is slightly narrower than the flash-induced ED EPR spectrum (Fig. 5). The broad spectral component in Fig. 5 seems to originate from weakly or non-interacting spins with 1/2 multiplicity. This signal presumably corresponds to separated polarons with non-equilibrium spin polarization. Such polarization can form



Scheme 3 Pulse sequence used in nutation experiments.

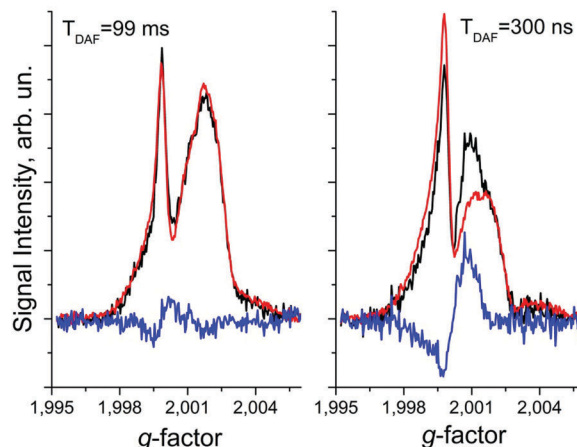


Fig. 7 Echo-detected EPR spectra used for the extracted SCPP signal. The left and right side plot shows spectra measured at  $T_{\text{DAF}} = 99 \text{ ms}$  and  $T_{\text{DAF}} = 300 \text{ ns}$  respectively. The red line shows a spectrum measured at a microwave power optimal for  $S = 1/2$ , the black line corresponds to the spectrum measured at the reduced microwave power. The first spectrum is multiplied with a coefficient  $K$  determined to minimize the difference (blue line) with the second spectrum for  $T_{\text{DAF}} = 99 \text{ ms}$ . Thus the difference between the two spectra measured at  $T_{\text{DAF}} = 300 \text{ ns}$  (blue line) corresponds to the SCPP signal which has a microwave power dependence deviating from that of  $S = 1/2$  species.

either due to spin evolution of geminate pairs during charge separation or by polarization transfer to the long-living free species.<sup>46,47</sup>

We measured the temperature dependence of the signal from the flash-induced species in the RR-P3HT/PC<sub>60</sub>BM composite (Fig. S3, ESI<sup>†</sup>) and found that the narrow central component of the spectrum due to the SCPP disappears upon increasing the temperature. Evidently, a SCPP forms at low temperature due to retardation of the charge separation process caused by the low thermal energy. The spectrum of polarized free species becomes narrower with increasing temperature because of partial averaging of the  $g$ -tensor anisotropy by fast molecular motions.

To determine the spin coupling parameters of the RR-P3HT<sup>•+</sup>/PC<sub>60</sub>BM<sup>•-</sup> SCPP we performed nutation experiments (Scheme 3). We measured nutations of the ESE signals of the separated polarons and of the SCPP (Fig. 9) at the maximum of the extracted SCPP signal ( $g = 2.00105$ ). The nutation signal of the SCPP was determined as the difference between the signal measured at  $T_{\text{DAF}} = 300 \text{ ns}$  and the microwave power of echo-forming pulses (the second and the third pulses in Scheme 3) corresponding to the maximum ESE intensity and the signal measured with the microwave power reduced by 6 dB multiplied by a coefficient  $K$  determined as described above. The amplitude of the nutation pulse (the first in Scheme 3) was kept the same during these measurements. The Microwave Pulse Forming Unit (MPFU) was used to keep the same amplitude of the nutation pulse and vary only the amplitude of echo-forming pulses. The nutation signal of the separated polarons was measured at  $T_{\text{DAF}} = 99 \text{ ms}$  where exclusively such spins were present. We applied a cosine Fourier transformation to experimental nutation curves and determined the nutation frequency of separated polarons at

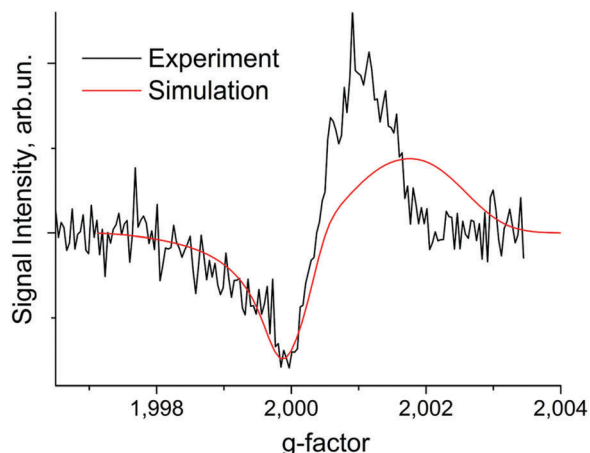


Fig. 8 Echo-detected EPR spectrum of the SCPP extracted for RR-P3HT/PC<sub>60</sub>BM at  $T_{\text{DAF}} = 300$  ns (black line). The red line shows the simulation done using the parameters of polaron species summarized in Table 1, dipolar interaction of 5 MHz, exchange interaction of 3 MHz.

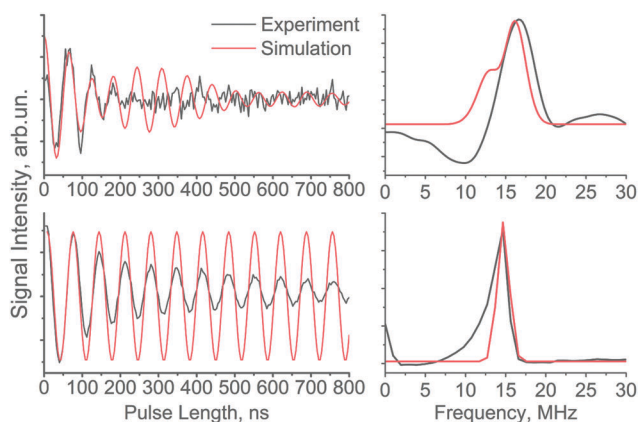


Fig. 9 Nutations of ESE signals in the RR-P3HT/PC<sub>60</sub>BM composite. The black lines show experimental data, the red lines correspond to simulations. Measurements were done at the maximum of the extracted SCPP ( $g = 2.00105$ ) using the three-pulse microwave sequence shown in Scheme 3. Durations of  $\pi/2$  and  $\pi$  echo-forming pulses are 20 ns and 40 ns, respectively, interpulse separation  $\tau = 400$  ns. The upper plot shows the signal of the SCPP extracted as described in the text, the simulation was done using the parameters of polaron species summarized in Table 1, dipolar interaction  $D = 5$  MHz, exchange interaction  $J = 3$  MHz. The lower plot corresponds to the signal of separated polarons at  $T_{\text{DAF}} = 99$  ms, the simulation was done using the parameters of the polarons summarized in Table 1 and zero magnetic interactions between polarons. The cosine Fourier representations of the experimental and simulated nutation curves are shown in the right part of the plot.

$T_{\text{DAF}} = 99$  ms and SCPPs, yielding 14.7 MHz and 16.6 MHz, respectively. Prior to Fourier transformation both experimental and simulated curves were zero-filled up to 1024 points and multiplied by the Gaussian apodization function  $f(x) = \exp(-(x/w)^2)$  with  $w = 200$  ns.

### Spectral simulations

We simulated the spectrum of the free species assuming that this spectrum consists of the contributions of two non-interacting

polarons RR-P3HT<sup>•+</sup> and PC<sub>60</sub>BM<sup>•-</sup> (Fig. 2). For the calculation we slightly modified the  $g$ -tensor values determined in ref. 29. We obtained the best agreement with our experimental data using  $g_{\text{RR-P3HT}^{\bullet+}} = [2.0028 \ 2.0020 \ 2.0009]$  and  $g_{\text{PC}_{60}\text{BM}^{\bullet-}} = [2.0001 \ 2.0001 \ 1.9985]$  and line widths of 9 MHz (3.2 G) and 4 MHz (1.4 G) for RR-P3HT<sup>•+</sup> and PC<sub>60</sub>BM<sup>•-</sup>, respectively. Also we included  $g$ -strain as the Gaussian shape distribution of  $g_{\text{RR-P3HT}^{\bullet+}}$  ( $y$ ) and  $g_{\text{PC}_{60}\text{BM}^{\bullet-}}$  ( $z$ ) with 0.0006 and 0.002 width, respectively. These values, summarized in Table 1, were used for all following calculations. All simulations were done using Matlab R2012b.

The simulation of the nutation experiment (Fig. 10) was done as described in the theory section in order to determine the strengths of magnetic interactions in the SCPP. The calculation was performed at the same  $g$ -value as in the experiment. From simulation of nutation traces with different  $J$  values we determined  $\omega_1 = 14.7$  MHz from the nutation frequency of the free paramagnetic species. We obtained that the exchange interaction in the SCPP is about 3 MHz. This result is in good agreement with  $J < 10$  MHz obtained using TR EPR.<sup>29</sup> Simulation of the nutation traces also allows us to estimate upper and lower limits of the exchange integral in the RR-P3HT<sup>•+</sup>/PC<sub>60</sub>BM<sup>•-</sup> SCPP, yielding  $1 \text{ MHz} < J < 5 \text{ MHz}$  (Fig. S4, ESI†). Evidently, the dipole interaction is also present in this SCPP, but its influence on the signal is much smaller than that of the exchange interaction; therefore it cannot be determined in the presence of a strong exchange interaction (Fig. S8, ESI†). We assumed  $D = 5$  MHz for the calculations, although it does not

Table 1 Simulation parameters for RR-P3HT<sup>•+</sup> and PC<sub>60</sub>BM<sup>•-</sup> polarons

	$g_x$	$g_y$	$g_z$	Line width
RR-P3HT <sup>•+</sup>	2.0028	2.0020	2.0009	9 MHz (3.2 G)
		$g$ -strain 0.0006		
PC <sub>60</sub> BM <sup>•-</sup>	2.0001	2.0001	1.9985	4 MHz (1.4 G)
			$g$ -strain 0.002	

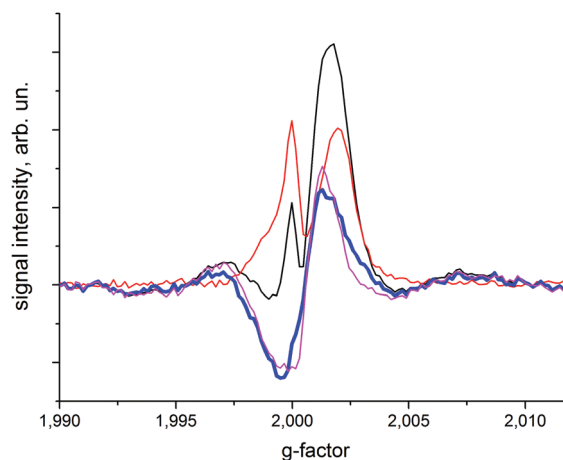


Fig. 10 ED EPR spectrum of the extracted SCPP for RR-P3HT/PC<sub>60</sub>BM at  $T_{\text{DAF}} = 300$  ns (thick blue line). ED EPR spectra for  $T_{\text{DAF}} = 300$  ns (black line),  $T_{\text{DAF}} = 99$  ms (red line) and flash-induced ED EPR spectrum calculated as their difference (magenta line).

influence the result of the calculation significantly. The upper limit of the dipolar interaction of  $D < 10$  MHz was derived previously from Q-band TR EPR,<sup>29</sup> which allows a rough estimation of the lower limit of the distances between the polarons in the SCPP giving 1.5 nm. Fast decay of the oscillations in the nutation pattern for the SCPP is probably caused by the distribution of  $J$  which was not taken into account in the present simulation.

We simulated the flash-induced ED EPR spectrum for the RR-P3HT/PC<sub>60</sub>BM composite as a sum of the spectra of non-interacting separated polarons and the singlet SCPP with the interaction (Fig. 5) determined from the nutation fitting described above. The contributions of separated polarons and the SCPP to the spectrum of flash-induced species in the RR-P3HT/PC<sub>60</sub>BM composite are comparable. Furthermore we calculated the theoretical “extracted SCPP spectrum” as a difference of the ESE calculated with a strong pulse and ESE calculated with a weak pulse, multiplied by  $2\sqrt{2}$  (Fig. 8), mimicking the protocol described in the Theory section. We can see from both spectra that the PC<sub>60</sub>BM<sup>•−</sup> signal at low  $g$ -values is reproduced quite well by our simulations, while in the RR-P3HT<sup>•+</sup> part (high  $g$ -values) the experimental and simulated spectra differ significantly. One of the possible reasons for this discrepancy is a correlation of the dipolar axis with the RR-P3HT<sup>•+</sup>  $g$ -tensor orientation for SCPP RR-P3HT<sup>•+</sup>/PC<sub>60</sub>BM<sup>•−</sup> which was not considered in the present calculations. Such correlation was taken into account and indeed led to a reasonable simulation of the RR-P3HT<sup>•+</sup>/PC<sub>60</sub>BM<sup>•−</sup> TR EPR spectrum at the X-band, although with a dramatically increased number of fitting parameters.<sup>23</sup> However, there is another possible reason for this discrepancy, which was not considered previously. It can be caused by the changes in the polymer  $g$ -tensor in the SCPP induced by the presence of an opposite charge in close proximity. Such an effect was observed also in nitroxide radicals.<sup>56</sup> This effect was confirmed using the quantum chemical  $g$ -factor calculation of the holes on the thiophene oligomer in the vicinity of the electron (Fig. S6, ESI†). The  $g$ -factors were computed with the TPSSh functional<sup>57,58</sup> and the def2-SVP basis set<sup>59,60</sup> using ORCA 4.0,<sup>61</sup> the spin-orbit coupling was computed using the SOMF(1X) approximation.<sup>62</sup> An increase in the spin delocalization along the chain as the point charge gets further away leads to an increase of the  $g$ -factors especially in the directions perpendicular to the polymer chain (Fig. S7, ESI†). We simulated the extracted SCPP spectrum with a modified RR-P3HT<sup>•+</sup>  $g$ -tensor [2.0012 2.0010 2.0009], the other parameters of polaron species are summarized in Table 1, dipolar interaction 5 MHz, exchange interaction 3 MHz, and obtained good agreement with the experiment (Fig. S8, ESI†). However, the  $g$ -value shift is higher than that predicted using quantum chemical calculations. We suggest that while the trend of the  $g$ -value change is correctly reproduced by DFT calculations, its magnitude is underestimated. It is known from high-field EPR that the largest principal  $g$ -value of RR-P3HT<sup>•+</sup> is sensitive to the P3HT environment: for RR-P3HT/PC<sub>60</sub>BM films it is larger by  $6 \times 10^{-4}$  than for toluene solution of RR-P3HT/PC<sub>60</sub>BM.<sup>63</sup> For this reason a strong change in the RR-P3HT<sup>•+</sup>  $g$ -tensor caused by negative PC<sub>60</sub>BM polarons in the vicinity is not surprising.

The significant  $J$  value for the RR-P3HT<sup>•+</sup>/PC<sub>60</sub>BM<sup>•−</sup> SCPP obtained in this work apparently contradicts the assumption of zero  $J$  in our previous study of out-of-phase ESE for this system.<sup>30</sup> We assume that this is caused by the very broad distribution of interspin distances in the RR-P3HT<sup>•+</sup>/PC<sub>60</sub>BM<sup>•−</sup> SCPP due to intrinsic disorder of the bulk heterojunction. For long distances  $J$  is close to zero and the dipolar interaction prevails; these pairs give a major contribution to the out-of-phase ESE. SCPPs with small interspin distances cannot be detected in out-of-phase ESE experiments because of the high modulation frequency. In this case ESE oscillations are lost within the spectrometer dead time. However, these pairs are observable in the ED EPR and nutation experiments described in the present study.

### RRa-P3HT/PC<sub>60</sub>BM composite

We also measured the signal of the SCPP in a similar composite of RRa-P3HT and PC<sub>60</sub>BM using the same procedure described in the Theory section. The observed signal of the extracted SCPP is significantly wider than that of the RR-P3HT/PC<sub>60</sub>BM composite (thick blue line in Fig. 10). Already from this nearly symmetric spectral shape a strong coupling between RRa-P3HT<sup>•+</sup> and PC<sub>60</sub>BM<sup>•−</sup> spins can be deduced. We found that the extracted SCPP spectrum for the RRa-P3HT/PC<sub>60</sub>BM composite is very similar to the usual flash-induced ED EPR spectrum (magenta line in Fig. 10). The difference between these two spectra is caused mainly by separated polarons with non-equilibrium polarization, which contribute to the latter spectrum and do not contribute to the former one, implying that their contribution is negligible. This is not surprising since light-induced charge separation in RRa-P3HT/PC<sub>60</sub>BM is relatively poor. Therefore, in contrast to the RR-P3HT/PC<sub>60</sub>BM composite, it was not necessary to use a special protocol for extracting the SCPP signal.

In order to determine the magnetic interaction parameters in the SCPP we measured its nutation and compared it with that of the long-living polarons measured at  $T_{\text{DAF}} = 99$  ms (Fig. 11). The signal of the SCPP was simply determined as a difference between signals measured at  $T_{\text{DAF}} = 300$  ns and  $T_{\text{DAF}} = 99$  ms. In both measurements the microwave power was reduced by 6 dB with respect to the optimal value for long-living polarons, to increase the relative contribution of the SCPP to the ESE signal. We applied cosine Fourier transformation for both curves zero-filled up to 1024 points and multiplied by the Gaussian apodization function  $f(x) = \exp(-(x/w)^2)$  with  $w = 500$  ns. The nutation frequencies were found to be 9.5 MHz for the SCPP and 7.2 MHz for the separated polarons. The nutation frequencies differ by approximately a factor of 1.32, meaning that the SCPP in this case is very similar to the purely triplet polaron pair, for which the value 1.41 is expected.<sup>50</sup> This means that in this composite the interaction between radicals in the pair is stronger than the typical difference in the Zeeman frequencies of RRa-P3HT<sup>•+</sup> and PC<sub>60</sub>BM<sup>•−</sup> at the Q-band, which is about 50 MHz. This result is in good agreement with the estimation of the dipolar coupling parameter (22 G) for RRa-P3HT<sup>•+</sup>/PC<sub>60</sub>BM<sup>•−</sup> derived from TR EPR data.<sup>23</sup> Similar to the present ESE results, the TR EPR spectrum of RRa-P3HT<sup>•+</sup>/PC<sub>60</sub>BM<sup>•−</sup> is much broader than that

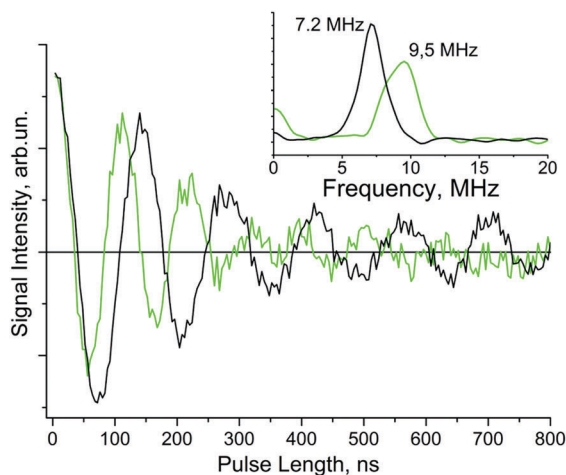


Fig. 11 Nutations of ESE signals in the RRa-P3HT/PC<sub>60</sub>BM composite. Black and green lines correspond to the signal of long-living polarons ( $T_{\text{DAF}} = 99$  ms) and flash-induced species (difference of the nutation traces at  $T_{\text{DAF}} = 300$  ns and  $T_{\text{DAF}} = 99$  ms). Measurements were done at the maximum of the extracted SCPP signal ( $g = 2.00105$ ). The cosine Fourier representation of the nutations is presented in the inset. The nutation frequencies differ by a factor of 1.32.

of RR-P3HT<sup>•+</sup>/PC<sub>60</sub>BM<sup>•-</sup>. This broadening is mainly caused by the increased strength of the dipolar interaction for RRa-P3HT<sup>•+</sup>/PC<sub>60</sub>BM<sup>•-</sup>, which reflects a smaller distance of charge separation due to a lack of regioregularity and  $\pi$ -conjugation loss in RRa-P3HT.

### Other composites

We compared the spectra of the flash-induced species measured both in low and high-efficient polymer/PC<sub>60</sub>BM composites using the pre-saturation pulse sequence (Scheme 2) to suppress the ESE signal of long-living polarons (Fig. 12). In all studied composites the flash-induced ESE signal consists of the same components (SCPP and non-equilibrium separated polarons), but the relative contributions of these species varied. The spectra of thermalized polarons in all these composites are similar: they consist of the PC<sub>60</sub>BM<sup>•-</sup> line at a lower  $g$ -value and the polymer polaron line at a higher  $g$ -value. However, the flash-induced ESE spectra of these composites differ significantly. We observed that the central narrow component corresponding to the SCPP (EPR spectral region between the peaks of PC<sub>60</sub>BM<sup>•-</sup> and polymer<sup>•+</sup>, shaded area in Fig. 12) is dominant in poorly performing MEHPPV/PC<sub>60</sub>BM and RRa-P3HT/PC<sub>60</sub>BM composites, comparable to the non-equilibrium separated polaron contribution in RR-P3HT/PC<sub>60</sub>BM and almost zero in high-efficient PTB7/PC<sub>60</sub>BM and PCDTBT/PC<sub>60</sub>BM composites. Importantly, the flash-induced ESE signal for PTB7/PC<sub>60</sub>BM and PCDTBT/PC<sub>60</sub>BM composites is almost solely formed by absorptively polarized separated PC<sub>60</sub>BM<sup>•-</sup> polarons and emissively polarized separated polymer polarons. This is confirmed by the nearly zero contribution of the SCPP to these spectra extracted according to the protocol in the Theory section (data not shown). Thus, the presence of the SCPP signal seems to be inversely correlated with the efficiency of the composite used as the active layer of the organic solar cell.

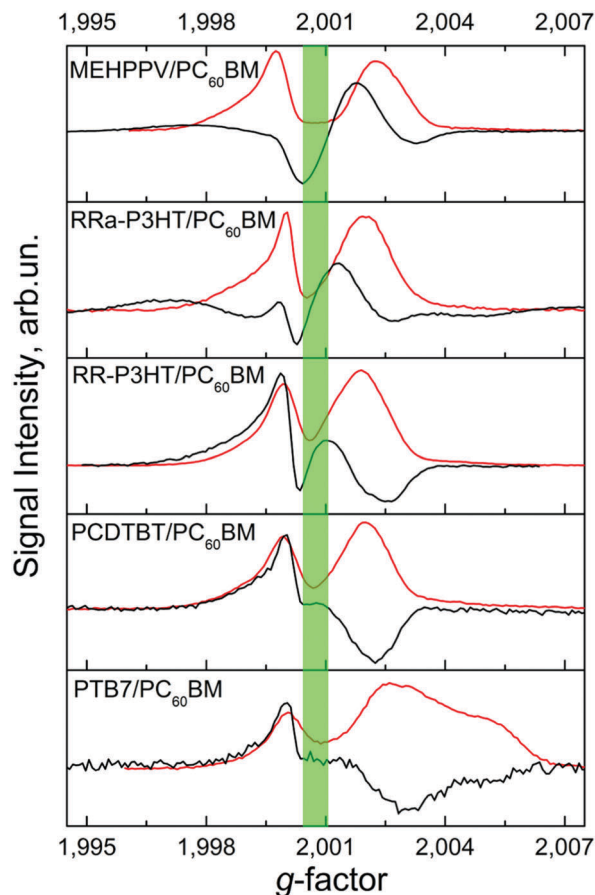


Fig. 12 Echo-detected EPR spectra of flash-induced species in different polymer/fullerene composites (black lines). The red lines show spectra of thermalized polarons measured under unsynchronized laser flash irradiation. The green shaded area indicates the region where the signal of thermalized polarons is weak and the SCPP signal dominates for composites of moderate efficiency.

## Conclusion

The light-induced charge separation in composites of different conductive polymers as electron donors and PC<sub>60</sub>BM fullerene as an acceptor was studied using pulse Q-band EPR spectroscopy at cryogenic temperatures. Since different pulse sequences can be applied and several experimental parameters can be varied (delays between microwave pulses, pulse amplitude and duration) this technique provides detailed information about the spin dynamics accompanying charge separation in such composites. Using these possibilities we managed to separate the contributions of different species to the in-phase flash-induced echo-detected EPR spectra. We found that the in-phase laser flash-induced EPR spectrum consists of several contributions:

- Charge transfer state, which is the spin-correlated polaron pair polymer<sup>•+</sup>/fullerene<sup>•-</sup>,
- Separated charges, which are the polaron pairs with negligible magnetic interactions and A/E spin polarization,
- Change of the spin polarization of pre-existing polarons in deep traps caused by the laser flash.

The latter contribution was not considered before. However, all of them are of importance for a correct interpretation of the flash-induced ESE signal in polymer/fullerene blends because they often have a comparable magnitude. It is expected that all these contributions are also present in the TR EPR spectra of polymer/fullerene composites, which are similar to some extent with respect to their in-phase flash-induced echo-detected EPR spectra.

A method for the determination of the strength of magnetic interactions between the polymer<sup>•+</sup> and fullerene<sup>•-</sup> spins using microwave nutation patterns is proposed. We simulated both the ESE nutation pattern and the ED EPR spectra of the RR-P3HT/PC<sub>60</sub>BM composite and found that an average exchange integral of about  $J = 3$  MHz for the SCPP in this composite. A nonzero dipolar interaction is expected in this case, but its value cannot be determined in the presence of strong exchange interactions. Species with such a relatively strong exchange interaction were not detected in previous out-of-phase ESE experiment on the RR-P3HT/PC<sub>60</sub>BM composite. Inconsistency of the interpretation of the experimental results obtained using different techniques (TR EPR, out-of-phase ESEEM and nutations) is probably caused by a broad distribution of the initial charge transfer distances.

The contribution of the SCPPs to the flash-induced ESE signal is high in composites with low-efficient polymers, while in composites with high-efficient polymers it is low. Thus the intensity of the SCPP ESE signal can be used to predict the charge separation efficiency in such composites. To analyze the charge separation efficiency quantitatively the distribution of CT states over the distance between polarons should be reconstructed from the ESE data, which is in progress now in our laboratories.

## Conflicts of interest

There are no conflicts of interest to declare.

## Acknowledgements

This work was supported by the Russian Foundation for Basic Research grant no. 15-03-07682 and 15-03-03242 and by Alexander von Humboldt Foundation research group linkage project “Light-induced processes and paramagnetic species in organic photovoltaics and photosynthesis”. The authors thank Dr A. G. Maryasov for helpful discussion of SCRP theory.

## References

- C. Deibel and V. Dyakonov, *Rep. Prog. Phys.*, 2010, **73**, 096401.
- K. A. Mazzio and C. K. Luscombe, *Chem. Soc. Rev.*, 2015, **44**, 78–90.
- J. Etxebarria, R. Ajuria and R. Pacios, *Org. Electron.*, 2015, **19**, 34–60.
- L. Lu, T. Zheng, Q. Wu, A. M. Schneider, D. Zhao and L. Yu, *Chem. Rev.*, 2015, **115**, 12666–12731.
- X. Liu, H. Chen and S. Tan, *Renewable Sustainable Energy Rev.*, 2015, **52**, 1527–1538.
- O. Ostroverkhova, *Chem. Rev.*, 2016, **116**, 13279–13412.
- M. A. Green, K. Emery, Y. Hishikawa, W. Warta, E. D. Dunlop, D. H. Levi and A. W. Y. Ho-Baillie, *Prog. Photovoltaics*, 2017, **25**, 3–13.
- B. Hemavathi, T. N. Ahipa and R. K. Pai, *Eur. Polym. J.*, 2015, **72**, 309–340.
- L. Dou, Y. Liu, Z. Hong, G. Li and Y. Yang, *Chem. Rev.*, 2015, **115**, 12633–12665.
- F. Meyer, *Prog. Polym. Sci.*, 2015, **47**, 70–91.
- L. Ying, F. Huang and G. C. Bazan, *Nat. Commun.*, 2017, **8**, 14047.
- R. Ganesamoorthy, G. Sathiyam and P. Sakthivel, *Sol. Energy Mater. Sol. Cells*, 2017, **161**, 102–148.
- C. B. Nielsen, S. Holliday, H.-Y. Chen, S. J. Cryer and I. McCulloch, *Acc. Chem. Res.*, 2015, **48**, 2803–2812.
- W. Chen and Q. Zhang, *J. Mater. Chem. C*, 2017, **5**, 1275–1302.
- J.-L. Bredas, J. E. Norton, J. Cornil and V. Copopceanu, *Acc. Chem. Res.*, 2009, **42**, 1691–1699.
- T. M. Clarke and J. R. Durrant, *Chem. Rev.*, 2010, **110**, 6736–6767.
- C. Deibel, T. Strobel and V. Dyakonov, *Adv. Mater.*, 2010, **22**, 4097–4111.
- F. Gao and O. Inganäs, *Phys. Chem. Chem. Phys.*, 2014, **16**, 20291–20304.
- S. Few, J. M. Frost and J. Nelson, *Phys. Chem. Chem. Phys.*, 2015, **17**, 2311–2325.
- A. J. Barker, K. Chen and J. M. Hodgkiss, *J. Am. Chem. Soc.*, 2014, **136**, 12018–12026.
- S. Gelinas, A. Rao, A. Kumar, S. L. Smith, A. W. Chin, J. Clark, T. S. van der Poll, G. C. Bazan and R. H. Friend, *Science*, 2014, **343**, 512–516.
- J. Behrends, A. Sperlich, A. Schnegg, T. Biskup, C. Teutloff, K. Lips, V. Dyakonov and R. Bittl, *Phys. Rev. B: Condens. Matter Mater. Phys.*, 2012, **85**, 125206.
- Y. Kobori, R. Noji and S. Tsuganezawa, *J. Phys. Chem. C*, 2013, **117**, 1589–1599.
- L. Franco, A. Toffoletti, M. Ruzzi, L. Montanari, C. Carati, L. Bonoldi and R. Po, *J. Phys. Chem. C*, 2013, **117**, 1554–1560.
- F. Kraffert, R. Steyrleuthner, S. Albrecht, D. Neher, M. C. Scharber, R. Bittl and J. Behrends, *J. Phys. Chem. C*, 2014, **118**, 28482–28493.
- J. Niklas, S. Beaupre, M. Leclerc, T. Xu, L. Yu, A. Sperlich, V. Dyakonov and O. G. Poluektov, *J. Phys. Chem. B*, 2015, **119**, 7407–7416.
- Y. Kobori and T. Miura, *J. Phys. Chem. Lett.*, 2015, **6**, 113–123.
- T. Miura, R. Tao, S. Shibata, T. Umeyama, T. Tachikawa, H. Imahori and Y. Kobori, *J. Am. Chem. Soc.*, 2016, **138**, 5879–5885.
- F. Kraffert and J. Behrends, *Mol. Phys.*, 2017, DOI: 10.1080/00268976.2016.1278479.
- E. A. Lukina, A. A. Popov, M. N. Uvarov and L. V. Kulik, *J. Phys. Chem. B*, 2015, **119**, 13543–13548.

- 31 E. A. Lukina, A. A. Popov, M. N. Uvarov, E. A. Suturina, E. J. Reijerse and L. V. Kulik, *Phys. Chem. Chem. Phys.*, 2016, **18**, 28585–28593.
- 32 M. N. Uvarov and L. V. Kulik, *Appl. Magn. Reson.*, 2013, **44**, 97–106.
- 33 M. N. Uvarov, A. G. Popov, E. A. Lukina and L. V. Kulik, *J. Struct. Chem.*, 2014, **4**, 644–650.
- 34 P. J. Hore, D. A. Hunter and C. D. McKie, *Chem. Phys. Lett.*, 1987, **137**, 495–500.
- 35 K. M. Salikhov, Y. E. Kandrashkin and A. K. Salikhov, *Appl. Magn. Reson.*, 1992, **3**, 199–216.
- 36 J. Tang, M. C. Thurnauer and J. R. Norris, *Chem. Phys. Lett.*, 1994, **219**, 283–290.
- 37 S. A. Dzuba, P. Gast and A. J. Hoff, *Chem. Phys. Lett.*, 1995, **236**, 595–602.
- 38 S. G. Zech, W. Lubitz and R. Bittl, *Ber. Bunsenges. Phys. Chem.*, 1996, **100**, 2041–2044.
- 39 H. Hara, S. A. Dzuba, A. Kawamori, K. Akabori, T. Tomo, K. Satoh, M. Iwaki and S. Itoh, *Biochim. Biophys. Acta*, 1997, **1322**, 77–85.
- 40 S. G. Zech, J. Kurreck, H. J. Eckert, G. Renger, W. Lubitz and R. Bittl, *FEBS Lett.*, 1997, **414**, 454–456.
- 41 A. Kamlowski, S. G. Zech, P. Fromme, R. Bittl, W. Lubitz, H. T. Witt and D. Stehlik, *J. Phys. Chem. B*, 1998, **102**, 8266–8277.
- 42 S. G. Zech, J. Kurreck, G. Renger, W. Lubitz and R. Bittl, *FEBS Lett.*, 1999, **442**, 79–82.
- 43 I. V. Borovykh, L. V. Kulik, S. A. Dzuba and A. J. Hoff, *Chem. Phys. Lett.*, 2001, **338**, 173–179.
- 44 P. J. Hore, *Mol. Phys.*, 1996, **89**, 1195–1202.
- 45 A. A. Popov, E. A. Lukina, L. Rapatskiy and L. V. Kulik, *J. Magn. Reson.*, 2017, **276**, 86–94.
- 46 P. J. Hore, D. J. Riley, J. J. Semlyen, G. Zwanenburg and A. J. Hoff, *Biochim. Biophys. Acta*, 1993, **1141**, 221–230.
- 47 M. T. Colvin, R. Carmiely, T. Miura, S. Richert, D. M. Gardner, A. L. Smeigh, S. M. Dyar, S. M. Conron, M. A. Ratner and M. R. Wasilewski, *J. Phys. Chem. A*, 2013, **117**, 5314–5325.
- 48 C. R. Timmel and P. J. Hore, *Chem. Phys. Lett.*, 1994, **226**, 144–150.
- 49 A. J. Hoff, P. Gast, S. A. Dzuba, C. R. Timmel, C. E. Fursman and P. J. Hore, *Spectrochim. Acta, Part A*, 1998, **54**, 2283–2293.
- 50 A. Schweiger and G. Jeschke, *Principles of Pulse Electron Paramagnetic Resonance*, Oxford University Press, New York, USA, 2005.
- 51 E. Reijerse, F. Lendzian, R. Isaacson and W. Lubitz, *J. Magn. Reson.*, 2012, **214**, 237–243.
- 52 J. M. Hodgkiss, S. Albert-Seifried, A. Rao, A. J. Barker, A. R. Campbell, R. A. Marsh and R. H. Friend, *Adv. Funct. Mater.*, 2012, **22**, 1567–1577.
- 53 S. van Reenen, M. V. Vitorino, S. C. J. Meskers, R. A. J. Janssen and M. Kemerink, *Phys. Rev. B: Condens. Matter Mater. Phys.*, 2014, **89**, 205206.
- 54 Y. Harima, T. Eguchi, K. Yamashita, K. Kojima and M. Shiotani, *Synth. Met.*, 1999, **105**, 121–128.
- 55 C. Corvaja, L. Franco, L. Pasimeni, A. Toffoletti and L. Montanari, *Chem. Phys. Lett.*, 1993, **210**, 355–361.
- 56 A. F. Gulla and D. E. Budil, *J. Phys. Chem. B*, 2001, **105**, 8056–8063.
- 57 J. Tao, J. P. Perdew, V. N. Staroverov and G. E. Scuseria, *Phys. Rev. Lett.*, 2003, **91**, 146401.
- 58 V. N. Staroverov, G. E. Scuseria, J. Tao and J. P. Perdew, *J. Chem. Phys.*, 2003, **119**, 12129.
- 59 F. Weigend and R. Ahlrichs, *Phys. Chem. Chem. Phys.*, 2005, **7**, 3297–3305.
- 60 F. Weigend, *Phys. Chem. Chem. Phys.*, 2006, **8**, 1057–1065.
- 61 F. Neese, *Wiley Interdiscip. Rev.: Comput. Mol. Sci.*, 2012, **2**, 73–78.
- 62 F. Neese, *J. Chem. Phys.*, 2005, **122**, 034107.
- 63 J. Niklas, K. L. Mardis, B. P. Banks, G. M. Grooms, A. Sperlich, V. Dyakonov, S. Beaupre, M. Leclerc, T. Xu, L. Yu and O. G. Poluektov, *Phys. Chem. Chem. Phys.*, 2013, **15**, 9562–9574.